Phase-dependent coherent population trapping and optical switching

J. Kou,[1,2] R. G. Wan,[1] Z. H. Kang,[1] L. Jiang,[1] L. Wang,[1] Y. Jiang,[1] and J. Y. Gao[1,*]

[1]*College of Physics, Jilin University, Changchun 130023, People's Republic of China*
[2]*Quantum Engineering Center, Beijing Institute of Control Device, Beijing 100854, People's Republic of China*

We propose a scheme for achieving phase-dependent coherent population trapping, showing that both the dark state of the atoms and light propagation dynamics depend on the relative phase of the fields. The atomic coherence prepared via adiabatic process plays a key role in the interaction of light with matter. And an optical switching based on the phase-controlled quantum interference is implemented, which may have potential application in high-speed optical communications and quantum information systems.

I. INTRODUCTION

Coherent population trapping (CPT) [1,2] refers to the phenomenon that the atom population is trapped in a superposition of lower states (so-called dark state) and the optical fields propagate through the medium without absorption via quantum interference. The significance of CPT is well illustrated by its numerous applications such as laser cooling [3], trapping of atoms in optical lattices [4], magnetometers [5], and atomic clocks [6].

In this paper, we propose and experimentally demonstrate a scheme to attain phase-dependent CPT in a three-level Λ-type atomic system, where the dark state is sensitive to the relative phase of the optical fields, so the light propagation dynamics exhibit a critical dependence on the input conditions. And one of the applications of this phenomenon is to implement an all-optical switching, which has been studied in many schemes [7–14] based on quantum interference in recent years.

The optical property in our scheme is similar to that presented in the system with closed-loop configuration, showing that both dynamics and the steady state of the atoms depend on the relative phase of the fields. However, our work is different from the former reports [15–20]; the phase-dependent CPT is observed in the closed-loop interaction schemes, which is formed by optical pulses separated in time, and the atomic coherence prepared via adiabatic process before the CPT step plays an important role in the interaction between optical fields and atoms. Furthermore, our experiment can be viewed as demonstrating the potential of this technique for achieving optical switching.

II. THEORY AND ANALYSIS

Figure 1(a) shows the energy-level structures of the ^{87}Rb D_1 transitions and the relevant laser coupling schemes used in the experiments. The temporal shapes of the coupling (2% of the real value) and switch (probe) pulses at the entrance of the Rb cell are shown in Fig. 1(b). The pulse widths (FWHM) of the coupling pulse (red curve) and the probe pulse (blue curve) are 450 and 15 ns, respectively, and the time interval T between the end edge of the coupling pulses and the peaks of the switch (probe) pulses is 65 ns. The coupling pulse with Rabi frequency

$\Omega_1(t)$ and the switch pulse with Rabi frequency $\Omega_s(t)$ are right circularly polarized; the second coupling pulse with Rabi frequency $\Omega_2(t)$ and the probe pulse with Rabi frequency $\omega_p(t)$ are left circularly polarized. All four lasers are resonant with the transition $|5S_{1/2}, F = 2\rangle \rightarrow |5P_{1/2}, F' = 1\rangle$ [as shown in Fig. 1(a)]. The Rabi frequencies of the end edge of the coupling pulses are assumed Gaussian with the amplitude envelopes of the form $\Omega_1(t) = \Omega_{10} \exp[-(t - 545)^2/13^2]$, $t \geqslant 545$ and $\Omega_2(t) = \Omega_{20} \exp[-(t - 545)^2/13^2]$, $t \geqslant 545$, where Ω_{10} and Ω_{20} denote the peak amplitudes of two coupling fields at the entrance of the vapor cell, respectively. Two strong coupling lasers establish a coherent superposition (dark state) of two lower states, given by

$$|\psi_D\rangle = \frac{\Omega_{20}}{\Omega}|1\rangle - \frac{\Omega_{10}}{\Omega}e^{i\varphi}|2\rangle, \tag{1}$$

where $\Omega = \sqrt{\Omega_{10}^2 + \Omega_{20}^2}$, and $\varphi = \varphi_2 - \varphi_1$ is the relative phase difference of the two coupling pulses. When the coupling lasers are turned off simultaneously, the amplitude and phase information is stored in the atomic coherence. The populations of the levels and atomic coherence right after the coupling fields being turned off are given as [the derivations of Eqs. (2) are reported in Appendix A]

$$\rho_{11} = \frac{\Omega_2^2}{\Omega_1^2 + \Omega_2^2},$$

$$\rho_{22} = \frac{\Omega_1^2}{\Omega_1^2 + \Omega_2^2}, \tag{2}$$

$$\rho_{12} = -\frac{\Omega_1\Omega_2}{\Omega_1^2 + \Omega_2^2}e^{i(\varphi_2-\varphi_1)}.$$

Then the switch and probe pulses are turned on; they are Gaussian pulses, with Rabi frequencies $\Omega_s(t) = \Omega_{s0} \exp[-(t - 610)^2/10^2]$ and $\Omega_p(t) = \Omega_{p0} \exp[-(t - 610)^2/10^2]$, respectively.

The optical fields and atomic superposition form a quasiloop configuration, where the quantum interference is dependent on the relative phase $\Delta\varphi = \varphi_1 - \varphi_2 - \varphi_S + \varphi_p$ and the amplitudes of applied optical fields [15–17], and we keep the condition in our experiment,

$$\frac{\Omega_{10}}{\Omega_{20}} = \frac{\Omega_{s0}}{\Omega_{p0}} = 1, \tag{3}$$

---

*jygao@mail.jlu.edu.cn
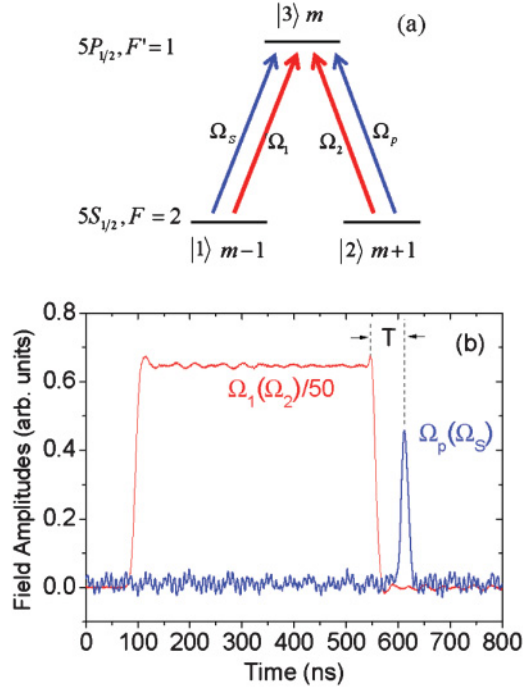
FIG. 1. (Color online) (a) Relevant energy level of ^{87}Rb atoms and laser excitation in the experiment. (b) The pulse sequence at the entrance of the Rb cell.

where the dynamics of probe pulse propagation can be effectively controlled by the relative phase, which can be modulated by each one of the four pulses in such a system.

We now turn to a theoretical discussion of this work, consider a three-level system [shown as Fig. 1(a)] in the rotating wave approximation, and assume an undepleted atomic coherence $\rho_{12} = -\Omega_{10}\Omega_{20}/(\Omega_{10}^2 + \Omega_{20}^2)e^{i(\varphi_2-\varphi_1)}$ prepared by two coupling pulses via adiabatic process before the probe (switch) pulses enter the sample. When the switch and probe pulses are turned on, the elements of the density matrix are given by the Liouville equation

$$\frac{d\rho_{31}}{dt} = i\Omega_s(t)\rho_{11}e^{i\varphi_S} + i\Omega_p(t)\rho_{21}e^{i\varphi_p} - \gamma_{31}\rho_{31},$$
$$\frac{d\rho_{32}}{dt} = i\Omega_p(t)\rho_{22}e^{i\varphi_p} + i\Omega_s(t)\rho_{12}e^{i\varphi_S} - \gamma_{32}\rho_{32}. \quad (4)$$

Here γ_{ij} $(i,j = 1,2,3)$ is the decoherence rate of the corresponding transition. The Maxwell equations for the fields are

$$\left(\frac{\partial}{\partial z} + \frac{1}{c}\frac{\partial}{\partial t}\right)\Omega_s(t)e^{i\varphi_S} = i\kappa_{13}\rho_{31},$$
$$\left(\frac{\partial}{\partial z} + \frac{1}{c}\frac{\partial}{\partial t}\right)\Omega_p(t)e^{i\varphi_p} = i\kappa_{23}\rho_{32}, \quad (5)$$

where $\kappa_{ij} = Nd_{ij}^2 w_{ij}/\varepsilon_0\hbar c$, N is the atomic density, and c is the speed of light in vacuum.

Equations (4) and (5) can be solved easily using the method in Ref. [21]; assuming that $\gamma_{31} = \gamma_{32} = \gamma$, $\kappa_{31} = \kappa_{32} = \kappa$, and

all four lasers are resonant with the corresponding transitions, the general solution of differential equations (4) and (5) is

$$\Omega_p(z,t) = -\Omega_s(0,t)|\rho_{12}|e^{i\Delta\varphi}\left[1 - \exp\left(\frac{\kappa z}{-\gamma}\right)\right]$$
$$+ \Omega_p(0,t)\left[\rho_{11} + \rho_{22}\exp\left(\frac{\kappa z}{-\gamma}\right)\right]. \quad (6)$$

The detailed theoretical calculations are given in Appendix B. By substituting Eq. (2) into Eq. (6), the expression of transmitted probe pulse reduces to

$$\Omega_p(z,t) = \frac{\Omega_2^2\Omega_p(0,t) + \Omega_1\Omega_2\Omega_s(0,t)e^{i\Delta\varphi}}{\Omega_1^2 + \Omega_2^2}$$
$$+ \frac{\Omega_1^2\Omega_p(0,t) - \Omega_1\Omega_2\Omega_s(0,t)e^{i\Delta\varphi}}{\Omega_1^2 + \Omega_2^2}\exp\left(-\frac{\kappa z}{\gamma}\right). \quad (7)$$

The physical origin of this optical switching can be understood by discussing how the relative phase affects the population and atomic coherence dynamics during the switching process.

The numerical solutions of Eqs. (4) and (5) are plotted in Fig. 2. The curves in Fig. 2(a) show the pulse shape in the time domain. The curves in Figs. 2(b) and 2(c) present the population of each level and the amplitude of coherence $|\rho_{12}|$. The initial population is equally distributed between state $|1\rangle$ and $|2\rangle$, and Rabi oscillation is clearly seen in the population of levels $|1\rangle$ ($|2\rangle$) and $|3\rangle$ when the two coupling lasers are applied. The coherence term $|\rho_{12}|$, as illustrated in Fig. 2, reaches its maximum value when states $|1\rangle$ and
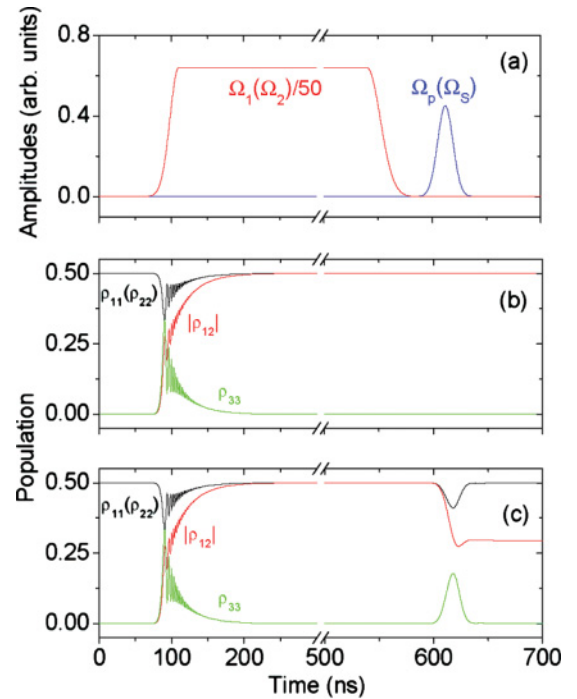
FIG. 2. (Color online) (a) The pulse shape in time domain. [(b) and (c)] Population transfer of levels $|1\rangle$, $|2\rangle$, and $|3\rangle$, and the amplitude of coherence $|\rho_{12}|$ between states $|1\rangle$ and $|2\rangle$ for the case of relative phase $\varphi = 0$ and $\varphi = \pi$, respectively.

$|2\rangle$ are half/half populated, with the dark state expressed in Eq. (1). Because the atoms in level $|3\rangle$ have a half chance of decaying to $|5S_{1/2}, F = 1\rangle$, a repumping beam from an external-cavity diode laser is tuned on resonant with the transition $|5S_{1/2}, F = 1\rangle \rightarrow |5P_{1/2}, F' = 2\rangle$ to pump the atoms back to $|5S_{1/2}, F = 2\rangle$ (not plotted in Fig. 1). The coupling lasers are adiabatically turned off after the system evolves into steady state, and the amplitude and phase information of coupling fields are stored in the form of atomic coherence; this process is similar to the fractional stimulated Raman adiabatic passage [22–25], which is a technique used to prepare coherent superposition states.

Then we turned on the switch and probe pulse simultaneously. Figure 2(b) shows that at $\Delta\varphi = 0$ the coherently prepared atoms are decoupled from the optical fields because of the destructive interference, so the light gets through the vapor cell without loss; this situation can be considered as coherent population trapping (CPT). To the contrary, for $\Delta\varphi = \pi$ [as shown in Fig. 2(c)], the phase condition for CPT is not satisfied and the instructive interference is dominant, the optical fields excite the atoms to the upper state, and the atoms absorb photons simultaneously. If $\kappa z \gg \gamma$, both of the switch and probe pulses are absorbed severely. The atoms decayed from the upper states are not localized in the dark state, so obviously the value of coherence $|\rho_{12}|$ decreases.

III. EXPERIMENT

The experimental apparatus is shown schematically in Fig. 3. The experiment is done in a 50-mm-long Rb vapor cell, which is magnetically shielded by μ metal and kept at 80 °C. Under normal conditions, the residual magnetic field is small, and the Zeeman effect on CPT in Rb atoms should not be appreciable. The laser from a CW single-frequency Ti:sapphire laser (Coherent 899) is split into two beams, which are turned on or off by an acousto-optic modulator according to the time sequence described below, respectively. One of the two beams is split again to generate two pulses as the coupling pulses $\Omega_1(t)$ and $\Omega_2(t)$, with linear orthogonal polarizations, and then are combined with a polarizing beam splitter. The other beam is also split into two beams: one as the probe pulse $\Omega_p(t)$ and the other as the switch pulse $\Omega_s(t)$; the switch pulse passes through an electro-optic modulator (EOM) and its phase is modulated by a voltage applied to the EOM. The two coupling pulses with approximately equal peak powers of 20 mW, and the peak power of the probe and switch pulses of 0.3 mW, propagate through a $\lambda/4$ wave plate, which results in an opposite circular polarization of the $\Omega_1(t)$ [$\Omega_p(t)$] and $\Omega_2(t)$
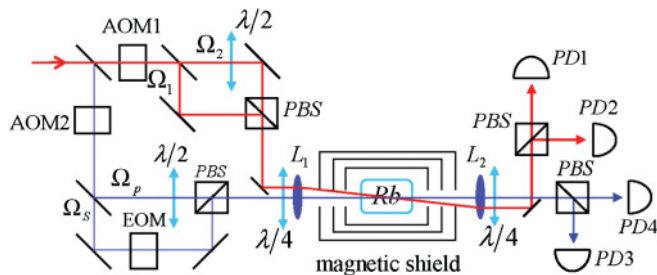
FIG. 3. (Color online) Schematic of the experimental setup.
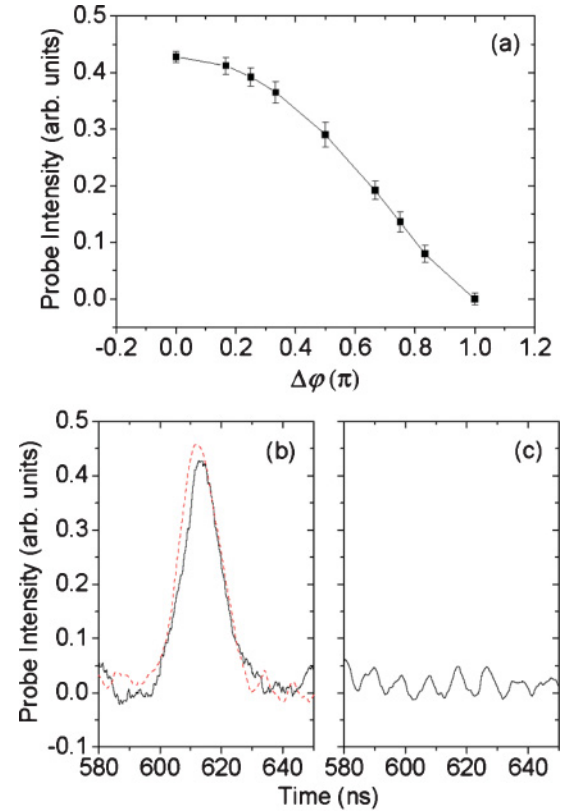
FIG. 4. (Color online) (a) Transmission of the control and the probe fields vs the variation of the relative phase. [(b) and (c)] The probe transmission in the condition of $\Delta\varphi = 2n\pi$ and $\Delta\varphi = (2n + 1)\pi$, respectively. The dashed curve in (b) is the input probe pulse as a reference.

$[\Omega_s(t)]$ pulses; then the four beams are focused by a lens (focus length 30 cm) into the atomic Rb vapor cell. After passing through the Rb cell, the pulses are directed to photodiodes, and are recorded by a digital oscilloscope (Tektronix TDS5104B).

Figure 4(a) displays the propagation dynamics along the medium for different values of the relative phase $\Delta\varphi$ of the system; $\Delta\varphi$ is adjusted by a sinusoidal voltage applied to the EOM. When the phase $\Delta\varphi$ varies from 0 to π, the light transmission also shows a sinusoidal variation. The solid line serves to guide the eye. In the case of the relative phase $\Delta\varphi = 2n\pi$ (n is integer), one sees that the probe pulse propagates through the medium as it was transparent; the theoretical analysis indicates that the atoms are decoupled from the optical fields because of destructive interference, so the output probe pulse (solid curve) almost persists in the Gaussian shape except for a little absorption at the raising edge compared with the input probe pulse (dashed curve), as shown in Fig. 4(b). In the $\Delta\varphi = (2n + 1)\pi$ situation, the coherent population trapping (CPT) condition is not satisfied, thus the probe pulse is absorbed severely by the atoms which jump to the upper state; the fluctuation shown in Fig. 4(c) is mainly electric noise from the environment. The experimental results coincide with Eq. (7), and also demonstrate the numerical simulation of population distribution in the previous section.

The particular situation shown in Figs. 4(b) and 4(c) can be applied for optical switching. The efficiency of the optical
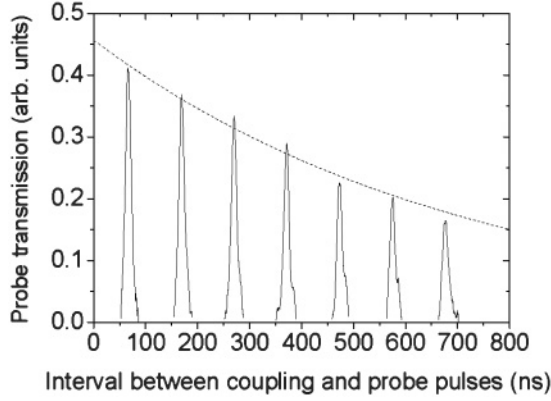
FIG. 5. The probe transmission observed in separate experiments that differ in the interval between coupling and probe/switch pulses.

switching can be defined as $\eta = (I_{\text{open}} - I_{\text{close}}) / I_{\text{in}}$. Here I_{in} is the input probe field intensity, I_{close} is the transmitted intensity when the switch is closed, and I_{open} is the transmitted intensity when the switch is open. In our experiments, when the switch is open (the destructive interference), the light transmission is $\approx 95\%$, which is limited by the absorption loss due to Zeeman broadening from the residual magnetic field and the decay rate of the ground state coherence; when the switch is closed (the instructive interference), the light transmission is $\approx 5\%$, which is limited by the optical depth of the atomic vapor. From the measurement, we derive that the observed switching efficiency is $\eta \approx 90\%$.

Since the atomic coherence is the key of optical switching, the effect induced by the dephasing of ground states should be considered. We turn on the probe pulse with different delay time T while keeping $\Delta\varphi = 0$. Figure 5 shows that destructive interference can occur even after a temporal delay between the coupling pulses and the probe (switch) pulses, but transmission of the probe pulse through the cell decreases with the increment in delay time. The probe intensity can be fit by a single exponential function (dashed curve in Fig. 5), and the decay time is 720 ns. The measured ground-state relaxation time, using the "phase control of EIT" method [26], is about 850 ns, which is close to the decay time estimated from the experimental data shown in Fig. 5. It should be mentioned that the proposed optical switching can also be carried out with two cw coupling fields, and the physical mechanism is the same as the experiment discussed above.

IV. CONCLUSION

In conclusion, phase-dependent coherent population trapping is observed in a three-level Λ-type atomic system. Such a scheme can be used to implement optical switching in which transmission and absorption of the probe pulse is controlled by the relative phase of optical fields. The switching speed depends on the durations and the intensities of the switch and probe pulses, and is not restricted by the relaxation rates. Numerical simulations have good agreement with the experimental observation.

APPENDIX A

The purpose of this Appendix is to show the derivation of Eq. (2). The atomic wave function can be written in the form

$$|\psi(t)\rangle = c_1(t)e^{-iw_1 t}|1\rangle + c_2(t)e^{-iw_2 t}|2\rangle + c_3(t)e^{-iw_3 t}|3\rangle. \tag{A1}$$

The probability amplitudes $c_k(t)$ of the three states $|k\rangle$ ($k = 1,2,3$) satisfy the Schrödinger equations

$$\begin{aligned}
\dot{c}_1 &= i\Omega_1(t)e^{i\varphi_1}c_3, \\
\dot{c}_2 &= i\Omega_2(t)e^{i\varphi_2}c_3, \\
\dot{c}_3 &= i[\Omega_1(t)e^{-i\varphi_1}c_1 + \Omega_2(t)e^{-i\varphi_2}c_2].
\end{aligned} \tag{A2}$$

In our experiment, all of the optical fields are resonant with the corresponding transition. In the steady-state condition, a solution of Eq. (A2) is given by

$$c_1 = \frac{\Omega_{20}e^{-i\phi_2}}{\sqrt{\Omega_{10}^2 + \Omega_{20}^2}}, \quad c_2 = \frac{-\Omega_{10}e^{-i\phi_1}}{\sqrt{\Omega_{10}^2 + \Omega_{20}^2}}, \quad c_3 = 0, \tag{A3}$$

where Ω_{10} and Ω_{20} denote the peak amplitudes of two coupling fields, respectively, and φ_1 and φ_2 are the phases of the two fields. The population distribution and atomic coherence between ground levels are given as

$$\begin{aligned}
\rho_{11} &= C_1^* C_1 = \frac{\Omega_{20}^2}{\Omega_{10}^2 + \Omega_{20}^2}, \\
\rho_{22} &= C_2^* C_2 = \frac{\Omega_{10}^2}{\Omega_{10}^2 + \Omega_{20}^2}, \\
\rho_{12} &= C_1^* C_2 = -\frac{\Omega_{10}\Omega_{20}}{\Omega_{10}^2 + \Omega_{20}^2}e^{i(\varphi_2 - \varphi_1)}.
\end{aligned} \tag{A4}$$

When the coupling fields attenuate simultaneously, keeping the value of $\Omega_1(t)/\Omega_2(t)$ constant, the trapping state does not change with time. Thus, the population distribution and atomic coherence between ground levels stay the same.

APPENDIX B

When the switch and probe pulses enter the sample, the elements of the density matrix are given by the Liouville equation

$$\begin{aligned}
\frac{d\rho_{31}}{dt} &= i\Omega_s(t)\rho_{11}e^{i\varphi_s} + i\Omega_p(t)\rho_{21}e^{i\varphi_p} - \gamma_{31}\rho_{31}, \\
\frac{d\rho_{32}}{dt} &= i\Omega_p(t)\rho_{22}e^{i\varphi_p} + i\Omega_s(t)\rho_{12}e^{i\varphi_s} - \gamma_{32}\rho_{32}.
\end{aligned} \tag{B1}$$

Here γ_{ij} ($i,j = 1,2,3$) is the decoherence rate of transition $|i\rangle \leftrightarrow |j\rangle$.

The Maxwell equations for the optical fields are

$$\left(\frac{\partial}{\partial z} + \frac{1}{c}\frac{\partial}{\partial t}\right)\Omega_s(t)e^{i\varphi_s} = i\kappa_{13}\rho_{31},$$
$$\left(\frac{\partial}{\partial z} + \frac{1}{c}\frac{\partial}{\partial t}\right)\Omega_p(t)e^{i\varphi_p} = i\kappa_{23}\rho_{32},$$
(B2)

where $\kappa_{ij} = Nd_{ij}^2 w_{ij}/\varepsilon_0\hbar c$, N is the atomic density, and c is the speed of light in vacuum.

We take Fourier transforms of Eqs. (B1) and (B2), and obtain

$$\frac{\partial}{\partial z}M_s = \left(\frac{i\kappa_{13}\rho_{11}}{-\omega - i\gamma_{31}} + \frac{i\omega}{c}\right)M_s + \frac{i\kappa_{13}\rho_{21}}{-\omega - i\gamma_{31}}M_p,$$
$$\frac{\partial}{\partial z}M_p = \left(\frac{i\kappa_{23}\rho_{22}}{-\omega - i\gamma_{32}} + \frac{i\omega}{c}\right)M_p + \frac{i\kappa_{23}\rho_{21}^*}{-\omega - i\gamma_{32}}M_s,$$
(B3)

where $M_{s(p)} = (1/2\pi)\int_{-\infty}^{+\infty}\Omega_{s(p)}(t)e^{i\omega t}\,dt$ is the Fourier transform of $\Omega_p(0,t)[\Omega_s(0,t)]$. Assuming that $\gamma_{31} = \gamma_{32} = \gamma$ and $\kappa_{31} = \kappa_{32} = \kappa$, the differential equation (B3) can be solved, yielding

$$M_p(z,\omega) = -M_s(0,\omega)|\rho_{12}|\,e^{i\Delta\varphi}e^{i\omega z/c}\left[1 - \exp\left(\frac{i\kappa z}{-\omega - i\gamma}\right)\right]$$
$$+ M_p(0,\omega)e^{iwz/c}\left[\rho_{11} + \rho_{22}\exp\left(\frac{i\kappa z}{-\omega - i\gamma}\right)\right].$$
(B4)

Here $\Delta\varphi = \varphi_1 - \varphi_2 - \varphi_S + \varphi_p$ is the relative phase of optical fields. Inverting the Fourier transformation in Eq. (B4) leads to

$$\Omega_p(z,t) = -\Omega_s(0,t)|\rho_{12}|\,e^{i\Delta\varphi}\left[1 - \exp\left(\frac{\kappa z}{-\gamma}\right)\right]$$
$$+ \Omega_p(0,t)\left[\rho_{11} + \rho_{22}\exp\left(\frac{\kappa z}{-\gamma}\right)\right].$$
(B5)

By substituting Eq. (A4) into Eqs. (B5) and (6) reduces to

$$\Omega_p(z,t) = \frac{\Omega_2^2\Omega_p(0,t) + \Omega_1\Omega_2\Omega_s(0,t)e^{i\Delta\varphi}}{\Omega_1^2 + \Omega_2^2}$$
$$+ \frac{\Omega_1^2\Omega_p(0,t) - \Omega_1\Omega_2\Omega_s(0,t)e^{i\Delta\varphi}}{\Omega_1^2 + \Omega_2^2}\exp\left(-\frac{\kappa z}{\gamma}\right).$$
(B6)

This expression can be viewed as the general solution, and is also given as the result in our original manuscript. Although Eq. (B6) contains Ω_1 and Ω_2, it still can be simplified in particular conditions. In our experiment, the amplitude condition $\Omega_1/\Omega_2 = \Omega_s/\Omega_p = 1$ is satisfied.

In the case of the relative phase $\Delta\varphi = 2n\pi$ (n is integer), Eq. (B6) reduces to

$$\Omega_p(z,t) = \frac{\Omega_2^2\Omega_p(0,t) + \Omega_1\Omega_2\Omega_s(0,t)}{\Omega_1^2 + \Omega_2^2} = \Omega_p(0,t),$$
(B7)

which shows that the probe pulse propagates through the medium without absorption.

While for $\Delta\varphi = (2n+1)\pi$, Eq. (B6) reduces to

$$\Omega_p(z,t) = \frac{\Omega_1^2\Omega_p(0,t) + \Omega_1\Omega_2\Omega_s(0,t)}{\Omega_1^2 + \Omega_2^2}\exp\left(-\frac{\kappa z}{\gamma}\right)$$
$$= \Omega_p(0,t)\exp\left(-\frac{\kappa z}{\gamma}\right),$$
(B8)

the amplitude of the probe pulse is attenuated exponentially, the decay rate of the probe field amplitude is dependent on the atomic vapor density and the cell length, when $\kappa z \gg \gamma$, and the probe pulse would be absorbed severely.

[1] G. Alzetta, A. Gozzini, L. Moi, and G. Orriols, Nuovo Cimento B **36**, 5 (1976).

[2] H. R. Gray, R. M. Whitley, and C. R. Stroud Jr., Opt. Lett. **3**, 218 (1978).

[3] A. Aspect, E. Arimondo, R. Kaiser, N. Vansteenkiste, and C. Cohen-Tannoudji, Phys. Rev. Lett. **61**, 826 (1988).

[4] A. Hemmerich, M. Weidemüller, T. Esslinger, C. Zimmermann, and T. Hänsch, Phys. Rev. Lett. **75**, 37 (1995).

[5] P. D. D. Schwindt, S. Knappe, V. Shah, L. Hollberg, J. Kitching, L.-A. Liew, and J. Moreland, Appl. Phys. Lett. **85**, 6409 (2004).

[6] S. A. Zibrov, I. Novikova, D. F. Phillips, R. L. Walsworth, A. S. Zibrov, V. L. Velichansky, A. V. Taichenachev, and V. I. Yudin, Phys. Rev. A **81**, 013833 (2010).

[7] S. E. Harris and Y. Yamamoto, Phys. Rev. Lett. **81**, 3611 (1998).

[8] D. A. Braje, V. Balic, G. Y. Yin, and S. E. Harris, Phys. Rev. A **68**, 041801 (2003).

[9] M. Yan, E. G. Rickey, and Y. F. Zhu, Phys. Rev. A **64**, 041801(R) (2001).

[10] C. Y. Ye, V. A. Sautenkov, Y. V. Rostovtsev, and M. O. Scully, Opt. Lett. **28**, 2213 (2003).

[11] Y. F. Chen, Z. H. Tsai, Y. C. Liu, and I. A. Yu, Opt. Lett. **30**, 3207 (2005).

[12] H. Kang, G. Hernandez, J. P. Zhang, and Y. F. Zhu, Phys. Rev. A **73**, 011802(R) (2006).

[13] J. P. Zhang, G. Hernandez, and Y. F. Zhu, Opt. Lett. **32**, 1317 (2007).

[14] V. A. Sautenkov, H. Li, Y. V. Rostovtsev, G. R. Welch, J. P. Davis, F. A. Narducci, and M. O. Scully, J. Mod. Opt. **55**, 3093 (2008).

[15] W. Maichen, F. Renzoni, I. Mazets, E. Korsunsky, and L. Windholz, Phys. Rev. A **53**, 3444 (1996).

[16] E. A. Korsunsky, N. Leinfellner, A. Huss, S. Baluschev, and L. Windholz, Phys. Rev. A **59**, 2302 (1999).

[17] E. A. Korsunsky and D. V. Kosachiov, Phys. Rev. A **60**, 4996 (1999).

[18] S. Kajari-Schröder, G. Morigi, S. Franke-Arnold, and G. L. Oppo, Phys. Rev. A **75**, 013816 (2007).

[19] N. Ph. Georgiades, E. S. Polzik, and H. J. Kimble, Opt. Lett. **21**, 1688 (1996).

[20] H. Li, V. A. Sautenkov, Y. V. Rostovtsev, G. R. Welch, P. R. Hemmer, and M. O. Scully, Phys. Rev. A **80**, 023820 (2009).

[21] A. Eilam, A. D. Wilson-Gordon, and H. Friedmann, Phys. Rev. A **73**, 053805 (2006).

[22] N. V. Vitanov, K. A. Suominen, and B. W. Shore, J. Phys. B **32**, 4535 (1999).

[23] V. A. Sautenkov, C. Y. Ye, Y. V. Rostovtsev, G. R. Welch, and M. O. Scully, Phys. Rev. A **70**, 033406 (2004).

[24] M. Oberst, F. Vewinger, and A. I. Lvovsky, Opt. Lett. **32**, 1755 (2007).

[25] X. L. Song, L. Wang, Z. H. Kang, R. Z. Lin, X. Li, Y. Jiang, and J. Y. Gao, Appl. Phys. Lett. **91**, 071106 (2007).

[26] V. A. Sautenkov, H. Li, Y. V. Rostovtsev, G. R. Welch, J. P. Davis, F. A. Narducci, and M. O. Scully, J. Mod. Opt. **56**, 975 (2009).